Drug Design, Development and Therapy

Dovepress
Taylor & Francis Group

Open Access Full Text Article

ORIGINAL RESEARCH

Antimicrobial Effects of *Kelisha* Capsule on *Escherichia coli* Induced Diarrhea in Mice

Guolin Shi[1,2], Xiao Lu[2], Guowei Wang[1], Kai Qian[2], Xiaokang Peng[2], Yangyang Zhu[2], Jiaxu Wu[2], Haiyong Ke[2], Li Chen[2], Yuanhang Zheng[2], Tao Yang[2], Xiaoying Shi[2], Pintong Huang[1,3,4]

[1]Department of Ultrasound in Medicine, The Second Affiliated Hospital of Zhejiang University School of Medicine, Zhejiang University, Hangzhou, 310009, People's Republic of China; [2]Post-Doctoral Research Center, Zhejiang SUKEAN Pharmaceutical Co., Ltd, Hangzhou, 311228, People's Republic of China; [3]Research Center of Ultrasound in Medicine and Biomedical Engineering, The Second Affiliated Hospital of Zhejiang University School of Medicine, Zhejiang University, Hangzhou, 310009, People's Republic of China; [4]Research Center for Life Science and Human Health, Binjiang Institute of Zhejiang University, Hangzhou, 310009, People's Republic of China

Correspondence: Pintong Huang, The Second Affiliated Hospital of Zhejiang University School of Medicine, Zhejiang University, 88 Jiefang Road, Shangcheng District, Hangzhou, 310009, People's Republic of China, Email huangpintong@zju.edu.cn

Background: *Kelisha* capsule (*KLSC*), listed in the Chinese Pharmacopoeia, has been employed for the treatment of infectious diarrhea. Nevertheless, the precise mechanism of *KLSC* remains to be elucidated.

Aim of the Study: This work was to investigate the antibacterial mode and therapeutic mechanism of *KLSC* towards *E. coli* infected diarrhea.

Materials and Methods: HPLC identified the primary chemical constituents of *KLSC*. A model of diarrhea was induced via *E. coli* injection. The impact of *KLSC* on *E. coli*-induced diarrhea was evaluated using a diarrhea score in Babl/c mice. The integrity of the intestinal barrier was assessed through staining and measuring levels of specific proteins. Furthermore, immunofluorescence staining was conducted to identify tight junction proteins in the small intestinal tissue. The full-length 16S rRNA was used to examine gut microbiota. Network pharmacology, molecular docking, and molecular dynamic simulation were used to investigate the impact of *KLSC* on diarrhea-related inflammation and quantify the expression levels of IL-6 and TNF-α in the blood and small intestine. The in vivo antibacterial activity and mode of action of *KLSC* were also investigated using IVIS imaging, transmission electron microscopy, scanning electron microscopy, and molecular dynamic simulation.

Results: *KLSC* exhibited a positive effect on *E. coli* infected diarrhea. The content of IL-6 and TNF-α in mice with *KLSC* was significantly reduced. Additionally, *KLSC* could restore the intestinal barrier function by reversing small intestine structure and up-regulating the expression of tight junction proteins. The *KLSC* significantly inhibit pathogenic bacteria and restore the gut microbiota diversity. IVIS Imaging System was visually observed significant antibacterial efficacy of *KLSC* in vivo. The *KLSC* disrupted the cell membrane system of *E. coli* through the interaction between bioactive molecule and bilayer.

Conclusion: *KLSC* normalized the gut barrier function, reshaped gut microbiota balance, suppressed the inflammatory pathways, and inhibited the bacterial activity, thereby relieving the diarrhea caused by *E. coli*.

Keywords: *Kelisha* capsule, diarrhea, antibacterial mechanism, molecular dynamics simulation, gut microbiota

Introduction

Diarrhea disease represents a significant public health concern, with a considerable burden of morbidity and mortality observed in infants and young children, particularly in developing countries.[1] As reported by the World Health Organization (WHO), *Escherichia coli* (*E. coli*) is one of the primary pathogens responsible for severe diarrhea in low-income countries.[2] Notwithstanding the considerable advances made in the field of sanitation, China remains one of the 15 countries with a high incidence of diarrhea.[3] Accumulating evidences demonstrated that the *E. coli* can cause a significant prevalence of intestinal disorders and diarrhea.[4–6] Antibiotics and immunomodulators are frequently employed in the treatment of *E. coli*-induced diarrhea. However, their effectiveness remains suboptimal and they can

Received: 18 December 2024
Accepted: 31 March 2025
Published: 10 April 2025

Graphical Abstract

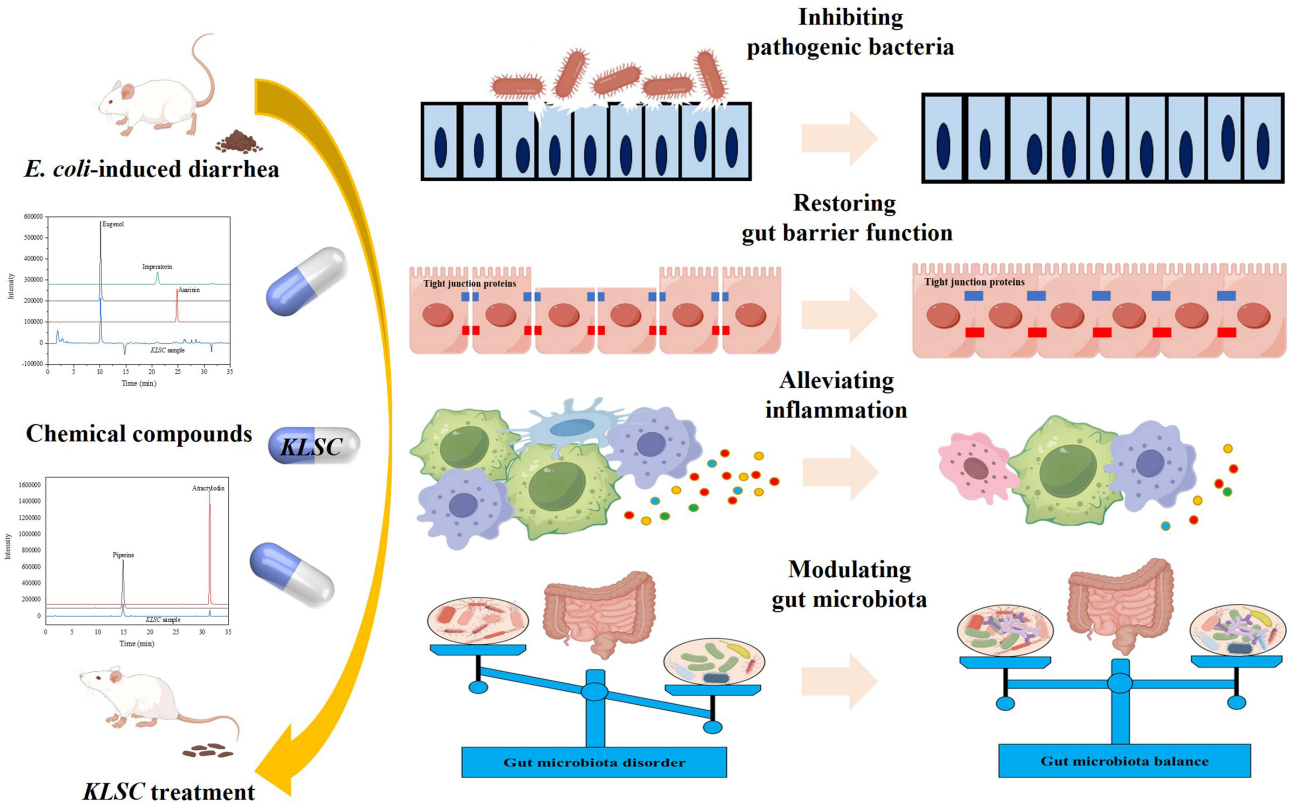

precipitate adverse effects such as antibiotic resistance, gastrointestinal dysfunction, or liver damage.[7] It is therefore necessary to identify alternative treatments for *E. coli*-infected diarrhea.

The practice of traditional Chinese medicine (TCM) has gained attention as a valuable source of medicine due to a number of factors, including its feasibility, synergistic effects, lower incidence of side effects, and higher biocompatibility in clinical applications.[8] *Kelisha* capsule (*KLSC*) is one of the TCM formulas that has been officially recorded in the Chinese Pharmacopoeia (*ChP* 2020). In clinical practice, *KLSC* has been employed for an extended period in the treatment of infectious diarrhea caused by *E. coli* in the Chinese mainland.

According to the published paper, *KLSC* exerts strong antibacterial effects on *E. coli* through disrupting the cell structure and affecting the energy metabolism process.[9] In the theory of TCM, it can show the efficacy of eliminating toxins and antidiarrheal by regulating *qi*.[10] *KLSC* include a variety of bioactive components, such as quercetin, piperine, eugenol, etc. Prior research has demonstrated the efficacy of quercetin in the treatment of infectious diarrhea caused by enteropathogenic *Escherichia coli* (*ETEC*).[11] It has been demonstrated that this compound can alleviate diarrhea and enhance intestinal barrier functions by increasing the expression of the TJPs and modulating the gut microbiota.[12] Piperine has been demonstrated to exert an anti-diarrhea effect through a variety of mechanisms, including the suppression of inflammatory responses.[13–15] Eugenol can mitigate inflammatory responses and preserve the barrier integrity of intestinal epithelial cells.[16] However, the current study only focuses on the anti-diarrheal effect of a single bioactive molecule, which is insufficient to reveal the mechanism of Chinese herbal formula. The potential therapeutic mechanism of *KLSC* remains unclear. In order to fill the study gap, it is imperative to investigate the potential action mechanism in alleviating *E. coli* infectious diarrhea.

In this study, the purpose is to elucidate the anti-diarrhea mechanism of *KLSC* from multiple dimensions. To achieve this goal, this work developed an *E. coli*-infected diarrhea model in Babl/c mice. Secondly, histopathological section and the expression levels of TJPs were quantified through immunofluorescence analysis to estimate the integrity of the intestinal barrier. Thirdly, the 16S rRNA was used to assess the impact of *KLSC* on the reshaping of gut microbiota. Furthermore, a network pharmacology, molecular docking and molecular dynamics (MD) simulation were employed to investigate the potential anti-inflammatory properties. Finally, the antibacterial effect was explored by IVIS Imaging System and MD simulation with in vivo and in vitro models. Together, the results elucidated that *KLSC* alleviated *E. coli*-induced diarrhea by regulating gut microbiota, improving intestinal barrier function, inhibiting inflammation and exerting an antibacterial action. This provided a solid basis and scientific proof for clinical application of *KLSC*.

Materials and Methods

Materials and Reagents

KLSC was provided by Zhejiang Sukean Pharmaceutical Co., Ltd. *KLSC* contains 12 types of Chinese herbal or mineral medicines, and it is displayed in supplementary material Table S1. Eugenol (CAS: 97–53-0), imperatorin (CAS: 482–44-0), asarinin (CAS: 133–04-0), piperine (CAS: 94–62-2), atractylodin (CAS: 55290–63-6) standard products were provided by China Academy of Food and Drug Administration.

Chemical Characterization of KLSC

The fingerprint of *KLSC* was identified through the utilization of an Agilent 1260 high Performance Liquid Chromatograph (Agilent, USA) with UV detection scheme. The DIKMA C-18 column (4.6 mm × 250 mm, 5 μm) was maintained a temperature of 30 °C. The mobile phases, designated A and B, were composed of acetonitrile and water, respectively. The elution process was detailed in Table 1. The flow rate was set at 1.0 mL/min. The wavelength of 280 nm was applied for the detection of eugenol, imperatorin and asarinin. And the wavelength of 340 nm was used to detect piperine and atractylodin. The HPLC methods used to characterize the chemical constituents of *KLSC* were validated in accordance with the standards set forth in the Chinese Pharmacopoeia.

Network Pharmacology and Molecular Dynamics Simulation Analysis

The main active chemical compounds of herbal medicines were screened in the Traditional Chinese Medicine System Pharmacology Database (TCMSP, https://old.tcmsp-e.com/tcmsp.php#). In the screening step, the bioactive compounds and corresponding putative protein targets were collected according to the oral bioavailability (OB ≥ 30%) and drug-like (DL ≥ 0.18).[17] The active components of mineral medicine in *KLS*C were screened from the HERB database (http://herb.ac.cn/). In addition, some active ingredients were also collected based on the literature. Potential targets of *E. coli*-induced diarrhea were searched from GeneCards database (https://www.genecards.org/) and Online Mendelian Inheritance in Man (OMIM). The intersection of the targets identified in *KLSC* and those associated with *E. coli*-induced diarrhea was obtained. These protein targets were then introduced into the STRING database (https://string-db.org/) for the construction of a protein-protein interaction (PPI) network. The key targets and compounds were then identified based on the PPI network. In order to investigate the interaction between active compounds and the key protein targets, the molecular docking was used to predict the binding affinity and conformation between core targets and active compounds as previously described in published papers.[18,19]

Table 1 The Elution Process Employed for KLSC

Time (min)	Proportion of A Phase (%)	Proportion of B Phase (%)
0	45	55
15	50	50
20	50	50
25	80	20
35	80	20

To further estimate the stability of the core protein target-active compound complexes, the Gromacs 2020 software was used for molecular dynamics (MD) simulation. In the MD, the core protein topologies and parameters were generated using the AMBER99SB-ILDN force field.[20] The force field parameters for active compounds were taken from the general AMBER force field (GAFF),[21] while the TIP3P model was used for water. The MD simulation process involves four steps: setup, energy minimization, equilibration, and simulation. A cubic box with a distance of 10 Å between the solute and the edge of the box was developed. The simulation system was neutralized by adding some sodium and chloride ions to mimic the natural condition. For energy minimization, the steepest descent algorithm was performed to minimize system energy with a maximum of 50,000 steps. Then the system was subjected to dual equilibration phases. Canonical ensemble (constant number of particles, volume, and temperature; NVT) with a temperature at 310 K and isobaric (the number of particles, pressure, and temperature; NPT) ensemble with a pressure at 101 kPa were carried out with 100 ps equilibration. After energy minimization and equilibration, the systems were subjected to run simulation for 50 ns, and the time step was 0.002 ps. All covalent bonds in the MD system were constrained through the LINCS algorithm.[22] The electrostatic interactions were calculated via Particle-mesh Ewald (PME)[23] scheme with a cut-off distance of 1.2 nm. At the end of the simulation, the root mean square deviation (RMSD) and radius of gyration (Rog) were calculated based on the output trajectory files. It could further understand the dynamic behavior and validate the stability of the core protein-active compound complexes under investigation.

Animal Experimental Design

All procedures involving animals adhered to the Guide for the Care and Use of Laboratory Animals issued by the National Institutes of Health and received ethical clearance from the Animal Ethical and Welfare Committee of Zhejiang SUKEAN Pharmaceutical Co., Ltd (Permission No. ZJSKA-IACUC-230801). Specific pathogen free (SPF) (SPF) Balb/c mice aged 6–8 weeks weighing about 20 g were maintained in a constant environment with a temperature of 25°C and humidity of 50% under a 12-hour light/dark cycle. Following a seven-day acclimatization period, 50 mice were randomly assigned to one of five groups (n = 10), comprising a control group, a model group, *KLSC* low dose (*KLSC-L), KLSC* high dose (*KLSC-H*), and ciprofloxacin (CPFX) group. CPFX was used as positive control group.

Prior to the administration of the bacterial solution, the mice were fasted for a period of 16 hours. The model group, *KLSC-L, KLSC-H*, and CPFX groups received a single intraperitoneal administration of *E. coli* suspension (0.2 mL, OD600 = 0.36). About 4 h after infection with *E. coli*, the mice showed diarrhea symptoms, such as supplementary material Figure S1 (a). At this time, the treatment groups were administered various concentrations of drug via intragastric administration. According to the clinical human dose, the animal equivalent dose was converted based on body surface area. The standard therapeutic dosage was used as *KLSC-L* (291.2 mg/kg) group, and *KLSC-H* (1456 mg/kg) group received pharmacological intervention at five-fold the standard therapeutic dosage. The positive control group was administered CPFX at 390 mg/kg. In a similar manner, the model and control groups were administered an equivalent volume of sterilized water via gavage. The mice were administered *KLSC* and CPFX for 4 days. The experimental steps were showed in Figure 1A. On the fourth day of treatment, the mice were placed in a sealed plastic box containing 5% isoflurane for 5 min,[24] and euthanized by cervical dislocation. Blood samples, fecal and intestinal tissue of all groups were collected according to the procedure of Figure 1A.

Evaluation of Diarrhea Score

Following the administration of the *E. coli*, the fecal data of each experimental group (n = 10) was duly recorded. As outlined in the published literature,[25] the degree of diarrhea was evaluated. The diarrhea scoring criterion was as follows and the stool scoring diagram was showed in supplementary material Figure S1. The severity of the diarrhea was assessed. The criteria for scoring diarrhea were as follows: A score of 0 was assigned to normal stools. Alterations in stool color or consistency resulted in a diarrhea score of 1. In the event of the presence of a wet tail or mucosa, the diarrhea score was equal to 2. The score for liquid stools was equal to 3. A score of 1 indicated the presence of diarrhea.

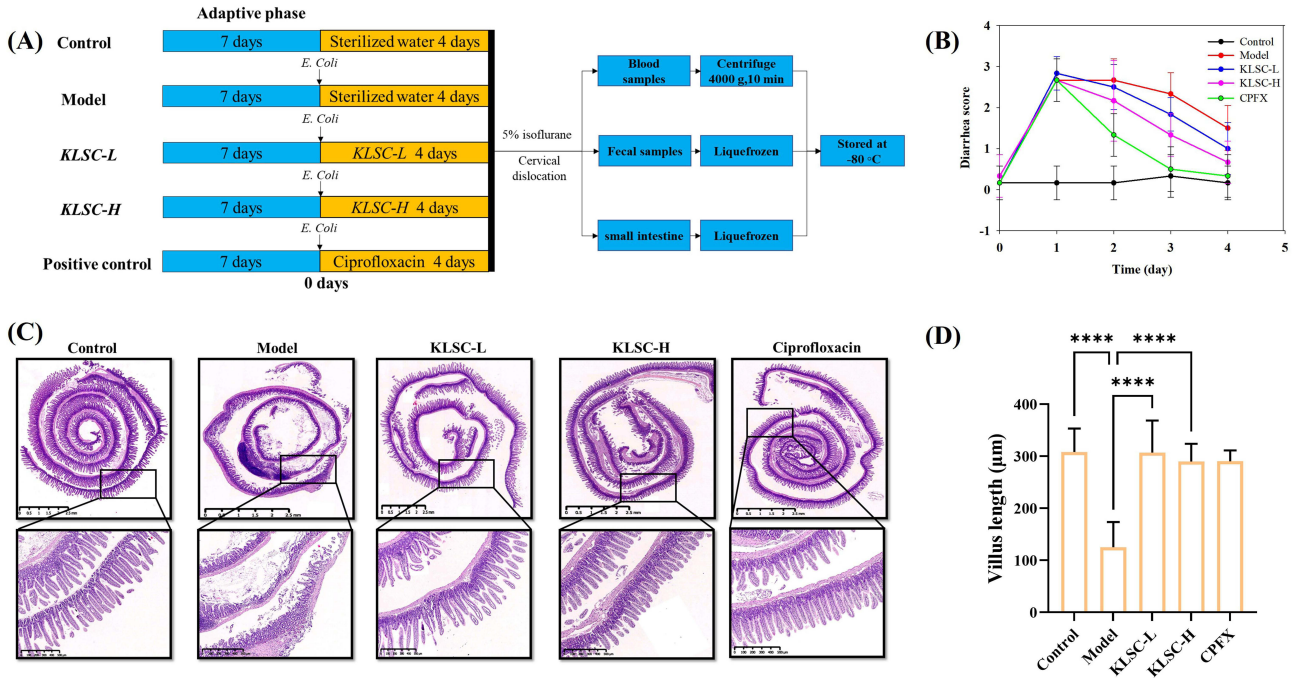

Figure 1 *KLSC* demonstrated the protective effect in mice with diarrhea. (**A**) The diagram illustrates the experimental steps. (**B**) The changes in diarrhea score. (**C**) The images of small intestine tissues stained with HE. (**D**) Villus lengths of various groups.

Histopathological Section and Immunofluorescence Staining Analysis

To evaluate the pathology of the intestine, the entire small intestine sample was fixed, embedded, and sliced. It was then stained with hematoxylin and eosin. The entire small intestine was examined under a light microscope.

Intestinal tight junction proteins (TJPs) are of significant importance in the context of gut physical barriers. For immunofluorescence staining, the small intestine tissue sections were embedded in paraffin after dewaxing and antigen repair. The sections were then incubated with an occludin primary antibody overnight at 4°C. Subsequently, the tissue sections were incubated with a fluorescence-labeled secondary antibody at room temperature. The same procedures were repeated for the incubation of the ZO-1 primary antibody. Subsequently, the tissue sections were subjected to DAPI staining, which enabled the observation of the nucleus. The resulting images were captured using a fluorescence microscope. Six independent samples in each group were observed under a microscope.

Measurement of Diamine Oxidase and Intestinal Trefoil Factor

There is a significant correlation between intestinal integrity and the occurrence of diarrhea. Diamine oxidase (DAO) and intestinal trefoil factor (ITF) serve as reliable indicators of intestinal permeability and integrity, respectively.[26] Consequently, in this study the DAO and ITF in the serum were measured by enzyme-linked immunosorbent assay (ADANTI. Inc., Wuhan, China). Each group was subjected to six independent repeated tests.

Inflammatory Factor Analysis

As indicated by the findings of network pharmacology, the levels of inflammatory factors were quantified through the use of an enzyme-linked immunosorbent assay (ELISA). The blood sample was centrifuged at 4°C and 4000 g for 10 minutes to obtain serum. The small intestine samples were lysed with lysis buffer. The intestinal tissue was broken with a tissue homogenizer. After centrifugation at 4000 g for 10 min at 4°C the supernatant was taken out for the detection of inflammatory factor. The levels of interleukin-6 (IL-6), tumor necrosis factor-α (TNF-α) were quantified in the serum and small intestine by the assay kit (Beyotime Biotech. Inc., Shanghai, China). All testing procedures were operated based on the supplier's instructions. Each group was subjected to six independent repeated tests.

https://doi.org/10.2147/DDDT.S511158

Analysis of Gut Microbiota

The fecal matter from each group (n = 6) was collected and stored at −80°C. The DNA was extracted from the fecal samples using the E.Z.N.A.® soil DNA Kit (Omega Bio-tek, Norcross, GA, USA). Subsequently, the samples were evaluated for quality, concentration, and purity using a NanoDrop 2000 spectrophotometer (Thermo Scientific, United States). The full-length 16S rRNA genes were amplified using the universal bacterial primers 27F (5'-AGRGTTYGATYMTGGCTCAG-3') and 1492R (5'-RGYTACCTTGTTACGACTT-3'). Following the PCR amplification, the resulting products were purified using the AMPure® PB beads (Pacific Biosciences, CA, USA) and quantified with the Qubit 4.0 (Thermo Fisher Scientific, USA) fluorometer. The barcoded amplicons were pooled in equimolar ratios and a DNA library was constructed using the SMRTbell Prep Kit 3.0 (Pacific Biosciences, CA, USA) in accordance with the instructions provided by the manufacturer. The purified SMRTbell libraries were subjected to sequencing on the PacBio Sequel IIe System (Pacific Biosciences, CA, USA). High-fidelity (HiFi) reads were obtained from the subreads, which were generated using circular consensus sequencing via SMRT Link v11.0. As detailed in the published literature,[27,28] the sequence data underwent processing and statistical analysis.

In vivo and in vitro Antibacterial Activity Against *E. Coli*

To visualize the impact of *KLSC* on *E. coli*, an IVIS Imaging System (PerkinElmer, USA) was employed to detect bioluminescent signals. The BALB/c nude mice comprising the model group, *KLSC* and CPFX groups were intraperitoneally administered 0.2 mL of bioluminescent *E. coli*. Two hours later, the *KLSC* was administered in accordance with the aforementioned procedure outlined in Section 2.4. To assess the antibacterial efficacy of *KLSC* in vivo, the signal intensity in mice was quantified at 0, 1, 2.5, and 5 h following *KLSC* administration. The photons emitted from the in vivo subjects were quantified using the IVIS imaging software. As qualitative detection data, three independent repeated tests were performed in each group.

To elucidate the antibacterial mechanism of *KLSC* against *E. coli*, an in vitro antibacterial experiment was conducted, as previously described in our published papers.[9] The bacterial samples of different groups were collected. The morphologies of various *E. coli* samples were analyzed by transmission electron microscopy (TEM, Hitachi HT7800, Japan) and scanning electron microscopy (SEM, Hitachi SU8100, Japan). As a qualitative observation, three independent replicate tests were performed in each group.

MD for Bioactive Molecules and *E. coli* Cell Membrane

In order to elucidate the interaction between the active molecules and the *E. coli* cell membrane, molecular dynamics (MD) simulations were employed to investigate the underlying mechanism. The active molecule selected for investigation was the representative component eugenol in *KLSC*. The *E. coli* membrane bilayer model comprised 42 lipid molecules of POPE, 12 molecules of POPG, and 3 molecules of cardiolipin (CL) in each leaflet. Additionally, the upper leaflet of the membrane bilayer was augmented with three molecules of peptidoglycan. The membrane bilayer model was developed by membrane builder facility of CHARMM-GUI.[29,30] The CHARMM36 force field, the GAFF and TIP3P model were used for membrane bilayer model, Eugenol and water, respectively.

Two modeling systems were employed in the molecular dynamics (MD) simulation. System 1, comprising eugenol and a membrane bilayer, was employed to investigate the interaction between the active molecule and the membrane structure. In the equilibrated lipid bilayer system, some water molecules were substituted with 100 Eugenol molecules via the GROMACS. After energy minimization, the NVT and NPT equilibration stages were performed at 101 kPa and 310 K for 100 ps, respectively. The systems were subjected to run simulation for 200 ns, and the time step was 2 fs. All covalent bonds in the MD system were constrained through the LINCS algorithm. The electrostatic interactions were calculated via Particle-mesh Ewald (PME) scheme with a cut-off distance of 1.2 nm. System 2, which included water and a membrane bilayer, was utilized as a control. The simulation parameters and process of system 2 were consistent with that of system 1. Following the 200 ns MD simulation, the interaction between eugenol and the membrane bilayer was analyzed and visualized.

Statistical Analysis

All experiment data were showed as the mean ± standard deviation (x ± SD). The test data were analyzed by software GraphPad Prism 9.0.0 (GraphPad Software Inc., CA, USA). Statistical analyses were performed using parametric or non-parametric approaches based on data distribution characteristics. For inter-group comparisons between two independent samples, Student's t-tests were applied under homogeneity of variance assumptions, with Welch's correction implemented when equal variances could not be assumed. Multigroup analyses involving three or more groups were conducted through one-way analysis of variance (ANOVA), followed by post hoc comparisons using the Dunnett T3 method to account for heterogeneous variances across groups. When fundamental assumptions of parametric testing (normality and homogeneity of variance) were violated, non-parametric alternatives including Mann–Whitney *U*-tests for pairwise comparisons and Kruskal–Wallis *H*-tests with Dunn-Bonferroni corrections for multiple groups were employed to ensure robust statistical inference. The $P < 0.05$ was taken to indicate statistical significance.

Results

Chemical Characterization

Figure S2 illustrated the HPLC fingerprints of *KLSC*. The main chemical constituents of *KLSC* were identified as atractylodin, piperine, eugenol, asarinin, and imperatorin based on the analysis of the peaks of standard products.

KLSC Improved Diarrhea Symptoms and Intestinal Damage

The control group of mice exhibited a favorable mental state, a typical diet, and normal stool patterns, displaying smooth and lustrous hair. In contrast, the mice in the model group exhibited a reduction in appetite, a depressed state, an arched back, and varying degrees of diarrhea. Notably, the diarrhea symptoms exhibited a marked improvement in the *KLSC* and CPFX groups in comparison to the model group (Figure 1B). Histological examination revealed notable differences in the intestinal tissue of the control and model groups, indicative of *E. coli*-induced intestinal damage (Figure 1C). As illustrated in Figure 1C and D, the villi length of the model group was significantly shorter than that of the control, *KLSC* and CPFX groups. Concomitantly, *KLSC* was observed to restore the density of villi, particularly in the high-dose group. *KLSC* group had comparable recovery effect with CPFX positive control group.

KLSC Suppresses the Inflammatory Response in Diarrhea Mice

In accordance with the tenets of network pharmacology, 82 active ingredients were identified from the TCMSP and HERB databases. Eugenol was included in the network pharmacology analysis due to its notable antibacterial efficacy.[31,32] Consequently, a total of 83 active components in *KLSC* were utilized for subsequent investigation. The key compounds with the highest degrees were identified as quercetin, kaempferol, β-sitosterol, stigmasterol, eugenol, and piperine, as illustrated in Figure 2A. The highest number of targets was obtained, and the following core targets were identified: TNF-α, IL-6, TP53, IL-1β, and JUN (Figure 2B). A KEGG pathway enrichment analysis was conducted, resulting in the identification of 167 enriched pathways. The 20 pathways with the lowest *p*-values were selected for further analysis and are presented in the supplementary material Figure S3. Signaling pathways such as the TNF signaling pathway (hsa04668) and the IL-17 signaling pathway (hsa04657) were found to be significantly enriched.

The AutoDock Vina was performed to calculate the binding energy of the key active compounds to core target proteins. Figure 2C illustrated a selection of representative three-dimensional binding conformations between active ingredients and protein targets. Notably, the binding energy between kaempferol and TNF-α was calculated to be −10.8 kcal/mol. Moreover, the binding energy between stigmasterol and IL-6 were less than −9 kcal/mol. Consequently, the complex, such as kaempferol-TNF-α, and stigmasterol-IL-6 underwent a 50 ns MD simulation. As displayed in Figure 2D, the RMSD value and Rog values illustrated slight fluctuations throughout the entire simulation period, indicating the presence of highly stable and compact protein structures.

The ELISA was employed to quantify the levels of inflammatory factors present in the serum and small intestinal tissue samples. The results were presented in Figure 3E and F. The results demonstrated that *E. coli* was capable of

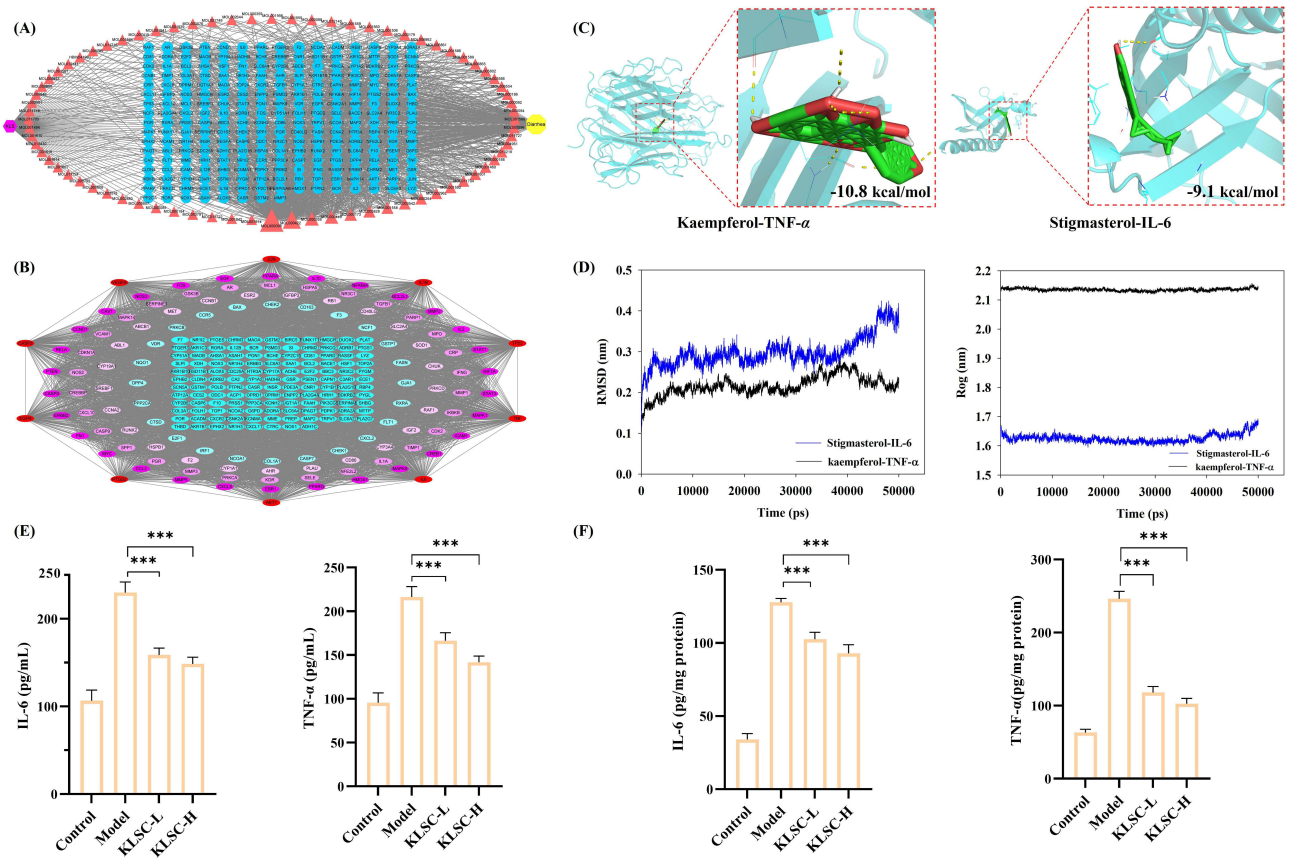

Figure 2 The in silico predictive outcomes of *KLSC*. (**A**) Prediction of key compounds of *KLSC*. (**B**) PPI network analysis. (**C**) Molecular docking of key ingredients and key targets. (**D**) Molecular dynamics simulation of key ingredients and key targets. (**E**) The contents of inflammatory factors in the serum. (**F**) The contents of inflammatory factors in the small intestine tissue.

markedly upregulating the expression of IL-6 and TNF-α. However, in comparison to the *E. coli*-infected group, the *KLSC* treatment showed a notable reduction in IL-6 and TNF-α expression levels.

KLSC Improves Intestinal Barrier Function in Diarrhea Mice

Intestinal tight junction proteins (TJPs) are integral components of the intestinal physical barrier, responsible for maintaining a complete and efficient gut barrier and preventing the invasion of pathogenic microorganisms.[33] To ascertain whether *KLSC* can improve the intestinal barrier function compromised by *E. coli*, the concentrations of DAO and ITF were analyzed, as showed in Figure 3A. The content of DAO in serum was increased in the model group, which reflected the impaired state of intestinal barrier integrity.[26] However, the levels of DAO were observed to be decreased in the *KLSC-L* and *KLSC-H* groups (Figure 3A). ITF plays a pivotal role in the preservation and restoration of intestinal mucosal integrity. From the Figure 3A, the content of serum ITF from *KLSC-L* and *KLSC-H* groups demonstrated an increase in comparison to the *E. coli*-induced diarrhea group. Furthermore, the results of immunofluorescence demonstrated that *E. coli* decreased the expression of TJPs ZO-1 and occludin, as displayed in Figure 3B. However, the administration of *KLSC* via oral route was observed to be significantly enhanced the TJPs expressions, specifically ZO-1 and occludin, as showed in the Figure 3B and C.

KLSC Ameliorates Gut Microbiota Diversity in *E. coli*-Induced Diarrhea Mice

The gut microbial community is closely associated with the occurrence of diarrhea, and gut microbial dysbiosis has been identified as a key factor in disrupting the intestinal barrier.[34] To reveal the alterations in the composition and function of the intestinal microbiota, the 16S RNA was used to characterize the gut microbiota profiles. A total of 1227267 optimized

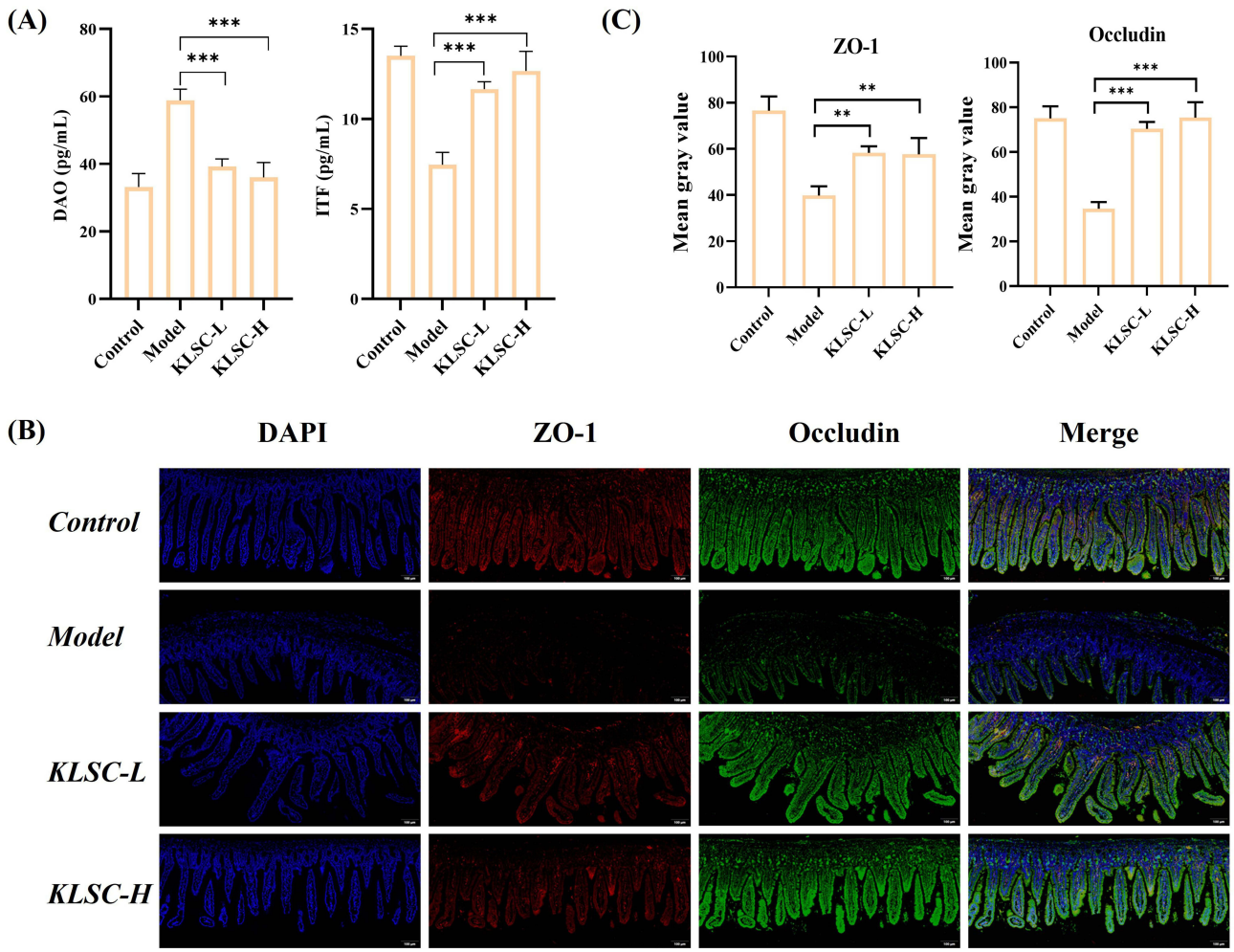

Figure 3 *KLSC* maintained small intestinal mucosal barrier function. (**A**) the contents of DAO and ITF. (**B**) Immunofluorescence analysis of tight junction proteins. (**C**) Quantitative analysis of ZO-1 and occludin expression levels.

sequences were acquired, with an average sequence length of 1498 bp. To assess the α-diversity of the gut microbiota, the intergroup rarefaction curves, Chao and Shannon indices were employed, as illustrated in Figure 4A–C. The rarefaction curves of the ASV level Sobs index showed that species diversity of each group reached a state of stability (Figure 4A), indicating that the amount of sequencing data was sufficient and reasonable.[35] As shown in Figures 5B and C, the Chao and Shannon indices of the model group exhibited a marked decline in comparison to those of the control group and *KLSC* treatment groups. Furthermore, *KLSC* was observed to be beneficial in improving the microbial dysbiosis index (Figure 4D). The β-diversity analysis revealed that the control, *KLSC-L*, and *KLSC-H* groups exhibited a closer distribution distance and shared similar characteristics, particularly the control and *KLSC-H* groups, as illustrated in the PCoA and NMDS score graphs (Figure 4E–F). It was noteworthy that the gut microbial composition of the model group was distinctly separated and distant from those of the other groups. Therefore, *KLSC* possessed the capability to modulate the intestinal microbiota and reinstated its diversity.

KLSC Regulates Gut Microbiota Structure in Diarrhea Mice

The study employed a multi-level taxonomic approach to assess the influence of varying doses of *KLSC* on the composition and structure of the gut microbiota. At the phylum level (Figure 5A), the control group was primarily composed of *Bacillota* (62.63%) and *Bacteroidota* (32.76%), while these accounted for only 18.32% and 27.65% in the model group. The abundance of *Pseudomonadota* in the model group exhibited a marked increase (53.95%). However,

https://doi.org/10.2147/DDDT.S511158

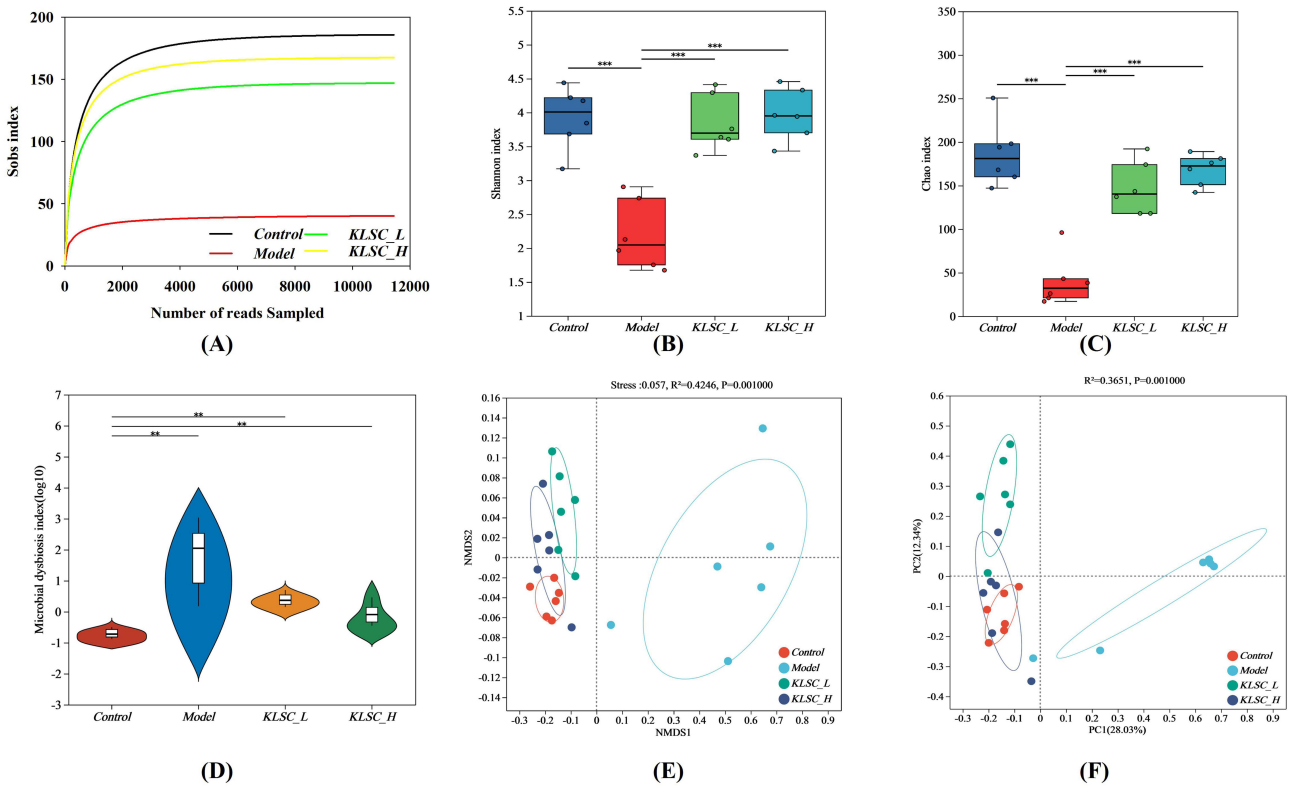

Figure 4 The structure and diversity of the gut microbiota in different groups. (**A**) Rarefaction curves. (**B**) Shamon index. (**C**) Chao index. (**D**) Microbial dysbiosis index. (**E**) PCoA score plots. (**F**) NMDS score plots.

following treatment with a high dosage of *KLSC*, the abundance of *Bacillota* and *Bacteroidota* was observed to recover to 61.09% and 35.68% respectively, which was found to be consistent with the control group. At the species level (Figure 5B), the administration of *E. coli* resulted in a notable elevation in the prevalence of pathogenic bacteria, including *E. coli* (53.79%) and *Enterococcus faecalis* (13.47%). Pearson's correlation analysis revealed a positive correlation between these pathogenic bacteria and both diarrhea symptoms and inflammatory factors (Figure 5C). However, in comparison to the group, the *KLSC* group demonstrated a notable reduction in pathogenic bacteria, namely *E. coli* and *Enterococcus faecalis*, accompanied by a striking increase in probiotics, specifically *Ligilactobacillus murinus* (Figure 5D–F). Furthermore, the gut microbial distribution at the species level and respective proportions in the *KLSC-H* group were found to be largely comparable to those observed in the normal group. The ten most abundant species, in descending order, were *Alistipes onderdonkii, Acetivibrio cellulolyticus, Ligilactobacillus murinus, Bacteroidetes bacterium RIFOXYB2_FULL_39_7, Acetivibrio aldrichii, Bacteroides uniformis*, unclassified_*g_Acetivibrio, Pseudoclostridium thermosuccinogenes, Kineothrix alysoides* and *Alistipes finegoldii*. As the main probiotics within the intestine, they exhibited a negative correlation with diarrhea score, inflammatory factors, and DAO (Figure 5C).

Antibacterial Mode of *KLSC* Against *E. coli*

The gut microbiota analysis indicated that *KLSC* could markedly suppress the proliferation of *E. coli*. This may be a significant factor in the alleviation of diarrhea. To further evaluate the in vivo antibacterial effect of *KLSC* on *E. coli*, the IVIS Imaging System was used to monitor the bioluminescent signal. In Figure 6A, the abdominal region exhibited a pronounced luminescent signal. In the case of the model group, the signal intensity exhibited an upward trajectory during the initial 2.5 h, reflecting the proliferation of *E. coli* in vivo. Subsequently, the signal declined, which may be attributable to the mice's immune response. Lower signal intensities were observed in the treatment group compared to the model group, indicating that *KLSC* exhibited a notable antibacterial effect in vivo.

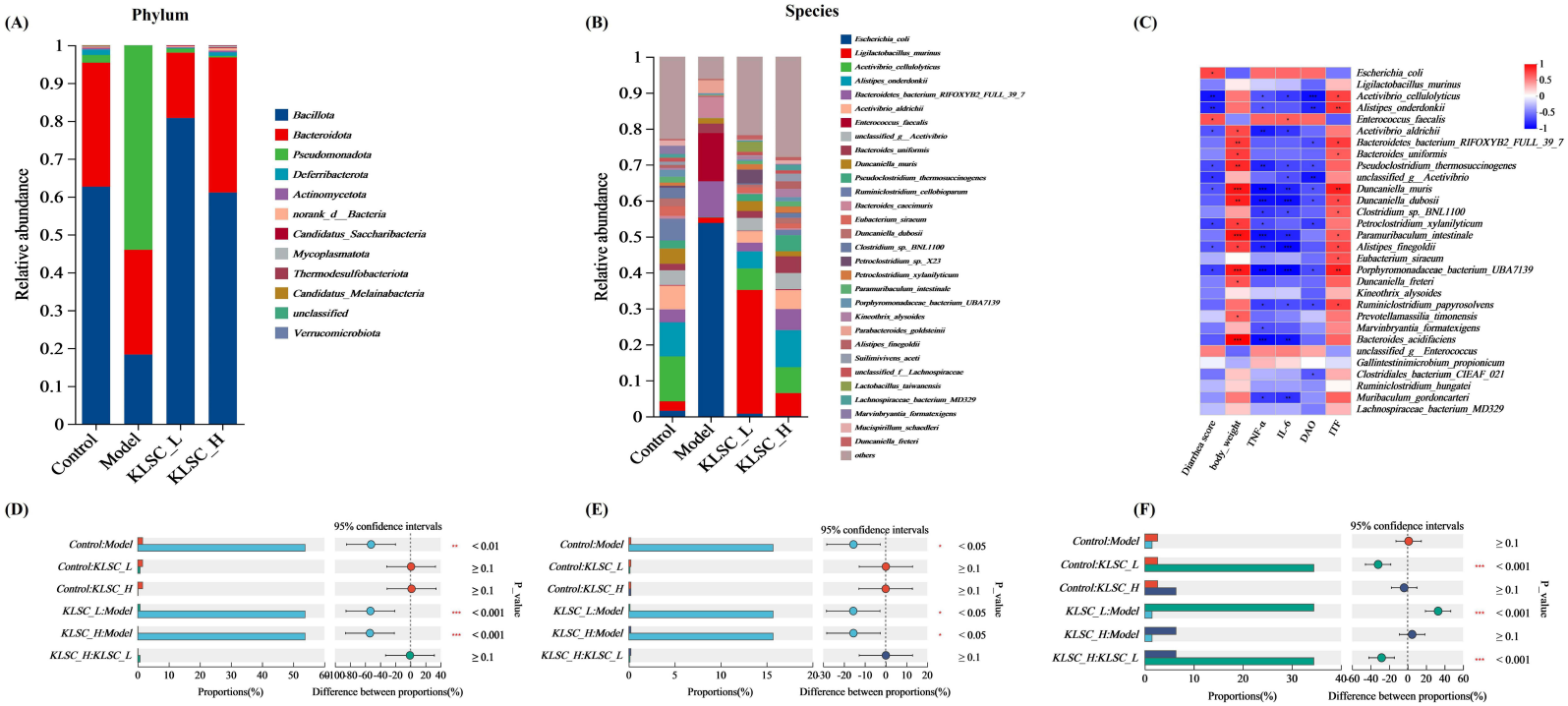

Figure 5 *KLSC* regulated compositions of gut microbiota. (**A**) Bar plot of community composition at the phylum level. (**B**) bar plot of community composition at species level. (**C**) Correlation analysis between microbiota and biochemically diarrhea traits. (**D–F**) Abundance changes of *Escherichia coli, Enterococcus faecalis, Ligilactobacillus murinus*.

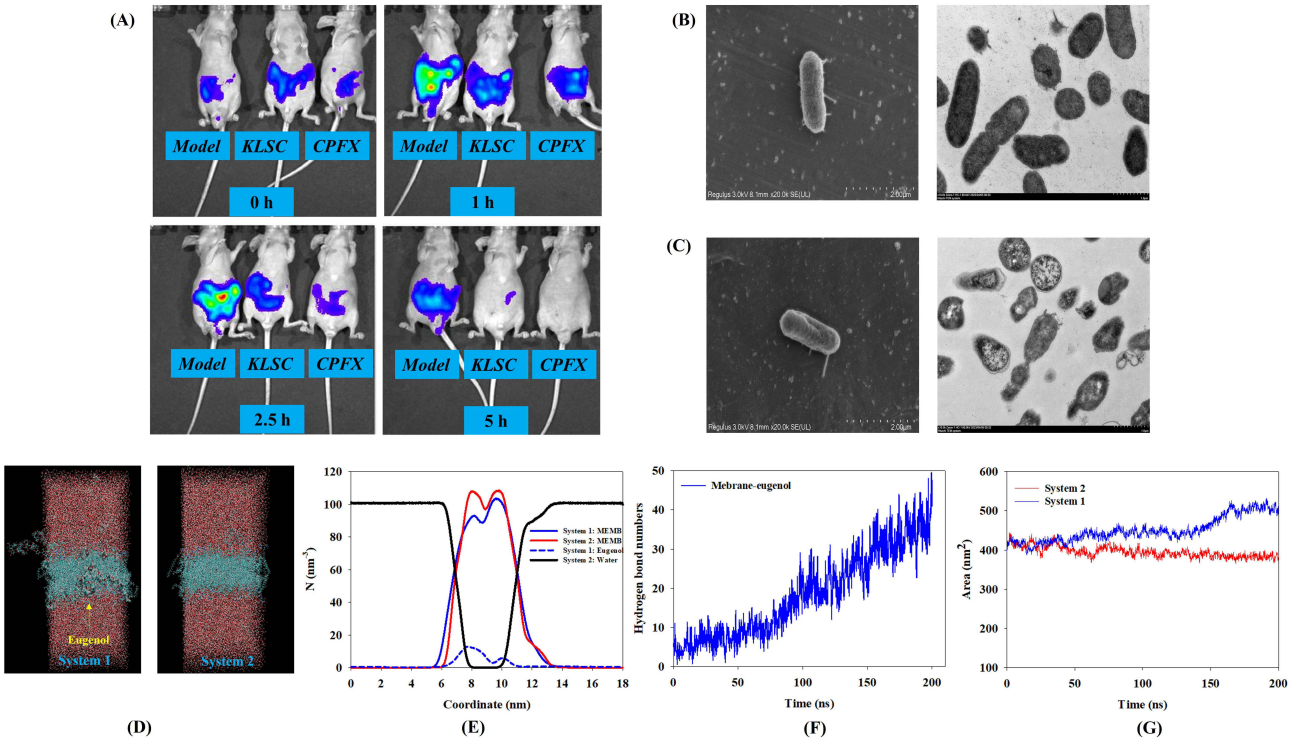

Figure 6 The antibacterial activity of *KLSC* in vivo and in vitro. (**A**) Monitoring the bioluminescent signal of *Escherichia coli*. (**B**) The images of SEM and TEM in control group. (**C**) The images of SEM and TEM in *KLSC* group. (**D**) Conformations of membrane model in different systems. (**E**) Density profiles of the bilayer. (**F**) Hydrogen bond numbers. (**G**) The surface area of the lipid bilayer.

The antibacterial mechanism of *KLSC* was investigated through the use of SEM, TEM and MD simulation. The control group displayed a typical surface and rod-shaped morphology with an intact membrane structure, and the cytoplasm was a homogeneous distribution (Figure 6B). However, the surface of the *E. coli* cells in the *KLSC* group exhibited clear distortion and irregularity, with notable deformation and collapse (Figure 6C). Moreover, *E. coli* cells treated with *KLSC* exhibited substantial damage, including a reduction in density, vacuolization, and distortion, as illustrated in Figure 6C. The antibacterial action of *KLSC* is evident from the disruption of the cell membrane. The MD simulation revealed that the active molecule eugenol in *KLSC* spontaneously inserts into the bilayer of *E. coli*, penetrating deeply into the bilayer model, as illustrated in the Figure 6D. This also resulted in a reduction the density of the bilayer, as illustrated in Figure 6E. Figure 6F illustrated that as eugenol interacted with the bilayer, the formation of hydrogen bonds increased, resulting in further damage to the bilayer structure. As displayed in Figure 6G, the surface area of the lipid bilayer gradually increased under the action of eugenol. The preceding analysis demonstrated that the membrane structure of the *E. coli* cell was disrupted.

Discussion

Diarrhea caused by the bacterium *E. coli* is a prevalent illness that have a significant impact on human health.[36] The *KLSC*, a classical TCM formula, has been employed extensively in clinical settings for the treatment of diarrhea. This study indicated that *KLSC* has the potential to alleviate *E. coli*-induced diarrhea through the suppression of inflammatory responses, the enhancement of intestinal barrier function, the modulation of gut microbiota, and the inhibition of bacterial growth.

Through the network pharmacology analysis, the key components were identified as quercetin, kaempferol, *β*-sitosterol, stigmasterol, eugenol, and piperine. *β*-sitosterol has been demonstrated to markedly diminish the levels of TNF-*α* and IL-6 contents in intestinal tissue of colitis mice.[37] Kaempferol alleviated dextran sulfate sodium (DSS) induced colitis by reducing level of IL-6 and TNF-*α*.[38] This work also demonstrated that *KLSC* decreased the expression

level of IL-6 and TNF-α. Based on the KEGG analysis, the AKT1, IL-6, TNF, JUN and IL-1β were significantly enriched in the TNF signaling pathway, IL-17 signaling pathway, and MAPK signaling pathway. In light of the published papers and network pharmacology, it can be posited that the bioactive compounds in *KLSC* can reduce the expression of IL-6 and TNF-α by regulating the inflammatory signaling pathway. This may be one of the reasons for relieving diarrhea.

TJPs are associated with the perijunctional cytoskeleton,[39,40] which plays a pivotal role in maintaining the integrity of the intestinal barrier and host health.[41] The maintenance of the mechanical barrier is contingent upon the normal expression of TJPs. The TJPs, including occludin and ZO-1, are utilized as pivotal biomarkers to assess intestinal barrier function and permeability. Abnormal expression of TJPs has been demonstrated to result in increased intestinal mucosal barrier permeability. A substantial body of literature exists indicating that *E. coli* can reduce the expression of TJPs, leading to the destruction of the barrier function.[42,43] In accordance with previously published research, this study also demonstrated that *E. coli* was capable of significantly reducing the expression levels of TJPs. As a reliable biomarker of intestinal mucosal integrity, an increase in DAO levels indicated a change in intestinal permeability.[44] The results demonstrated that the intestinal barrier function of mice was significantly impaired in the model group. However, this study observed that *KLS*C effectively enhanced TJPs expression levels and reduced DAO contents. Moreover, the structure of the small intestine, which is responsible for absorbing nutrients and water, was notably restored by *KLSC*. Based on the published paper, the piperine and eugenol have the function of regulating TJPs and repairing the tight junction damage.[45–48] According to the HPLC results, it was known that *KLSC* capsules contained piperine and eugenol. It suggests that these bioactive components in the *KLSC* may regulate reverse the down-regulation of TJPs expression levels and restore the small intestine structure. These findings indicates that *KLSC* may alleviate *E. coli*-infected diarrhea by normalizing intestinal barrier function.

The composition of the intestinal flora is a critical factor in human health and the development of disease.[49,50] In recent years, a substantial body of research has indicated that an imbalance in the gut microbiota is a significant contributing factor to bacterial diarrhea.[51] This study demonstrated that the diversity and richness of the intestinal flora were significantly reduced in mice with *E. coli*-infected diarrhea, a finding that was consistent with previously published results.[52] Furthermore, the relative abundance of *E. coli* and *Enterococcus faecalis* exhibited a marked increase in the model group during the *E. coli* invasion. Modifying the composition of the gut microbiota may prove an effective means of alleviating intestinal inflammation and reducing the incidence of diarrhea.[7,53] As evidenced by the PoCA and NMDS analysis, the gut microbiota distribution following *KLSC* treatment was found to be closely aligned with that of the normal group. Notably, the distribution of intestinal flora in the *KLSC-H* group exhibited a high degree of overlap with that of the normal group. Some active compounds, such as piperine and eugenol, have been shown to regulate intestinal flora.[54,55] This may be the reason why *KLSC* reshapes gut microbiota. As previously demonstrated, regulating the composition and balance of the gut microbiota can improve diarrhea caused by *E. coli* infection.[56,57] Therefore, *KLSC* might be have the potential to alleviate diarrhea by reversing the disruption of the gut microbiota.

Furthermore, *KLSC* may also exert antibacterial effects in vivo. *E. coli* is capable of producing two principal categories of enterotoxins, namely heat-stable enterotoxins (ST) and heat-labile toxin (LT).[58] Both toxins have the potential to disrupt the integrity of TJPs in intestinal epithelial cells, alter the internal environment of the liquid, and stimulate the excessive secretion of body fluids and electrolytes.[51] In this study, it was observed that the active molecules of *KLSC* were capable of disrupting the cell membrane system of *E. coli* through interactions with the bilayer structure, as evidenced by molecular dynamics simulations. Therefore, the inhibition of *E. coli* activity may result in a reduction in enterotoxin production. A reduction in enterotoxins was observed to be beneficial in preventing *E. coli* from damaging the integrity of the intestine. It is an effective way to alleviate the symptoms of diarrhea. In this article, the IVIS Imaging System was employed to visually observe that *KLSC* exhibited significant in vivo antibacterial efficacy. The results indicated that *KLSC* could potentially alleviated diarrhea by inhibiting the activity of *E. coli* and mitigating the negative effects of *E. coli*.

However, there are some limitations in this work. For example, the mechanism by which *KLSC* up-regulates tight junction proteins is unclear. This study has clearly found that *KLSC* can regulate intestinal flora, but the regulatory pathway has not been studied. It is necessary to further explore in future.

Conclusion

In conclusion, the potential mechanism of *KLSC* alleviating *E. coli*-induced diarrhea was elucidated through various ways, such as restoring the intestinal barrier function, regulating multiple inflammation, modulating the gut microbiota and inhibiting *E. coli* cell growth. Compared to antibiotics and probiotics, the most prominent difference is that *KLSC* integrates "antibacterial, anti-inflammatory, intestinal tissue repair and gut flora regulation" to alleviate diarrheal symptoms, rather than focusing on a single target. This multi-pathway approach is conducive to delaying the emergence of drug resistance. These findings provided scientific evidence to support the clinical application of *KLSC*.

Abbreviations

DAO, Diamine oxidase; *E. coli*, *Escherichia coli*; ELISA, Enzyme-linked Immunosorbent Assay; HE, Hematoxylin-Eosin; HPLC, High-Performance Liquid Chromatography; IL-6, Interleukin-6; ITF, Intestinal trefoil factor; *KLSC*, *Kelisha* capsule; *KLSC-H*, *KLSC* high dose; *KLSC-L*, *KLSC* low dose; SEM, Scanning electron microscopy; TCM, Traditional Chinese medicine; TEM, Transmission electron microscopy; TJPs, Tight junction proteins; TNF-α, Tumor Necrosis Factor-α; MD, Molecular dynamics.

Data Sharing Statement

The datasets used and/or analyzed during the current study are available from the corresponding author upon reasonable request.

Animal Ethics Statement

All procedures involving animals adhered to the Guide for the Care and Use of Laboratory Animals issued by the National Institutes of Health and received ethical clearance from the Animal Ethical and Welfare Committee of Zhejiang SUKEAN Pharmaceutical Co., Ltd (Permission No. ZJSKA-IACUC-230801).

Acknowledgment

The author would like to thank all the participating members.

Funding

This work was supported by the National Natural Science Foundation of China (NO. 82030048), the Science and Technology Co-construction Project of National TCM Comprehensive Reform Demonstration Zone (NO. GZY-KJS-ZJ-2025-026, Key Research and Development Program of Zhejiang Province (NO. 2019C03077), and supported by the Zhejiang SUKEAN Pharmaceutical Co., Ltd (RD23-01).

Disclosure

All authors disclosed no relevant relationships. The authors report no conflicts of interest in this work.

References

1. Liu L, Oza S, Hogan D, et al. Global, regional, and national causes of child mortality in 2000–13, with projections to inform post-2015 priorities: an updated systematic analysis. *Lancet*. 2015;385(9966):430–440. doi:10.1016/S0140-6736(14)61698-6
2. World Health Organization. Diarrhoeal Disease. 2024. Available from: https://www.who.int/en/news-room/fact-sheets/detail/diarrhoeal-disease. Accessed 13, January 2024.
3. Walker CLF, Rudan I, Liu L, et al. Global burden of childhood pneumonia and diarrhoea. *Lancet*. 2013;381(9875):1405–1416. doi:10.1016/S0140-6736(13)60222-6
4. Ledwaba SE, Costa DV, Bolick DT, et al. Enteropathogenic Escherichia coli infection induces diarrhea, intestinal damage, metabolic alterations, and increased intestinal permeability in a murine model. *Front Cell Infect Microbiol*. 2020;10:595266. doi:10.3389/fcimb.2020.595266
5. Sandle GI. Infective and inflammatory diarrhoea: mechanisms and opportunities for novel therapies. *Curr Opin Pharmacol*. 2011;11(6):634–639. doi:10.1016/j.coph.2011.09.005
6. Bolick DT, Medeiros PHQS, Ledwaba S, et al. Critical role of zinc in a new murine model of enterotoxigenic Escherichia coli diarrhea. *Infect Immun*. 2018;86(7). doi:10.1128/iai.00183-18
7. Yue Y, He Z, Zhou Y, et al. Lactobacillus plantarum relieves diarrhea caused by enterotoxin-producing Escherichia coli through inflammation modulation and gut microbiota regulation. *Food Funct*. 2020;11(12):10362–10374. doi:10.1039/D0FO02670K

8. Dai R, Sun Y, Su R, Gao H. Anti-Alzheimer's disease potential of traditional Chinese medicinal herbs as inhibitors of BACE1 and AChE enzymes. *Biomed Pharmacother*. 2022;154:113576. doi:10.1016/j.biopha.2022.113576
9. Shi G, Lu X, Zheng Y, et al. Insights into the potential dual-antibacterial mechanism of Kelisha capsule on Escherichia coli. *BMC Complement Med Therap*. 2024;24(1):207. doi:10.1186/s12906-024-04500-7
10. Liu S, Zhao Y, Li C, et al. Long-term oral administration of Kelisha capsule does not cause hepatorenal toxicity in rats. *J Ethnopharmacol*. 2024;332:118320. doi:10.1016/j.jep.2024.118320
11. Hirudkar JR, Parmar KM, Prasad RS, et al. The antidiarrhoeal evaluation of Psidium guajava L. against enteropathogenic Escherichia coli induced infectious diarrhoea. *J Ethnopharmacol*. 2020;251:112561. doi:10.1016/j.jep.2020.112561
12. Xu B, Qin W, Xu Y, et al. Dietary quercetin supplementation attenuates diarrhea and intestinal damage by regulating gut microbiota in weanling piglets. *Oxid Med Cell Longev*. 2021;2021.
13. Afroz M, Bhuia MS, Rahman MA, et al. Anti-diarrheal effect of piperine possibly through the interaction with inflammation inducing enzymes: in vivo and in silico studies. *Eur J Pharmacol*. 2024;965:176289. doi:10.1016/j.ejphar.2023.176289
14. Taqvi SIH, Shah AJ, Gilani AH. Insight into the possible mechanism of antidiarrheal and antispasmodic activities of piperine. *Pharm Biol*. 2009;47 (8):660–664. doi:10.1080/13880200902918352
15. Shamkuwar PB, Shahi SR. Study of antidiarrhoeal activity of piperine. *Der Pharmacia Lettre*. 2012;4(1):217–221.
16. Hui Q, Ammeter E, Liu S, et al. Eugenol attenuates inflammatory response and enhances barrier function during lipopolysaccharide-induced inflammation in the porcine intestinal epithelial cells. *J Anim Sci*. 2020;98(8). doi:10.1093/jas/skaa245
17. Zhang W, Tian W, Wang Y, et al. Explore the mechanism and substance basis of Mahuang FuziXixin Decoction for the treatment of lung cancer based on network pharmacology and molecular docking. *Comput Biol Med*. 2022;151(Pt A):106293. doi:10.1016/j.compbiomed.2022.106293
18. Ko M, Kim Y, Kim HH, et al. Network pharmacology and molecular docking approaches to elucidate the potential compounds and targets of Saeng-Ji-Hwang-Ko for treatment of type 2 diabetes mellitus. *Comput Biol Med*. 2022;149:106041. doi:10.1016/j.compbiomed.2022.106041
19. Shen X, Zhang W, Peng C, et al. In vitro anti-bacterial activity and network pharmacology analysis of Sanguisorba officinalis L. against Helicobacter pylori infection. *Chin Med*. 2021;16(1):33. doi:10.1186/s13020-021-00442-1
20. Lindorff-Larsen K, Piana S, Palmo K, et al. Improved side-chain torsion potentials for the Amber ff99SB protein force field. *Proteins Struct Funct Bioinf*. 2010;78(8):1950–1958. doi:10.1002/prot.22711
21. Wang J, Wolf RM, Caldwell JW, Kollman PA, Case DA. Development and testing of a general amber force field. *J Comput Chem*. 2004;25 (9):1157–1174. doi:10.1002/jcc.20035
22. Hess B, Bekker H, Berendsen HJ, Fraaije JG. LINCS: a linear constraint solver for molecular simulations. *J Comput Chem*. 1997;18 (12):1463–1472. doi:10.1002/(SICI)1096-987X(199709)18:12<1463::AID-JCC4>3.0.CO;2-H
23. Darden T, York D, Pedersen L. Particle mesh Ewald: an N· log (N) method for Ewald sums in large systems. *J Chem Physics*. 1993;98 (12):10089–10092.
24. Ko MJ, Mulia GE, Van Rijn RM. Commonly used anesthesia/euthanasia methods for brain collection differentially impact MAPK activity in male and female C57BL/6 mice. *Front Cell Neurosci*. 2019;13:96. doi:10.3389/fncel.2019.00096
25. Yu H, Wang Y, Zeng X, et al. Therapeutic administration of the recombinant antimicrobial peptide microcin J25 effectively enhances host defenses against gut inflammation and epithelial barrier injury induced by enterotoxigenic Escherichia coli infection. *THE FASEB Journal*. 2020;34 (1):1018–1037. doi:10.1096/fj.201901717R
26. Ren S, Wang C, Chen A, Bai Z, Tian Y, Lv W. Lactobacillus paracasei influences the gut-microbiota-targeted metabolic modulation of the immune status of diarrheal mice. *Food Funct*. 2023;14(9):4368–4379.
27. Huo W, Hu T, Shao Y, Ye R, Muhammad A, Lu W. Enhanced food waste chain elongation for caproate production: role of inorganic carbon and optimization strategies. *Resour Conserv Recycl*. 2024;203:107439. doi:10.1016/j.resconrec.2024.107439
28. Xu L, Sun L, Zhang S, Wang S, Lu M. High-resolution profiling of gut bacterial communities in an invasive beetle using PacBio SMRT sequencing system. *Insects*. 2019;10(8):248. doi:10.3390/insects10080248
29. Jo S, Kim T, Iyer VG, Im W. CHARMM-GUI: a web-based graphical user interface for CHARMM. *J Comput Chem*. 2008;29(11):1859–1865. doi:10.1002/jcc.20945
30. Jo S, Cheng X, Lee J, et al. CHARMM-GUI 10 years for biomolecular modeling and simulation. *J Comput Chem*. 2017;38(15):1114–1124. doi:10.1002/jcc.24660
31. Jeyakumar GE, Lawrence R. Mechanisms of bactericidal action of Eugenol against Escherichia coli. *J Herbal Med*. 2021;26:100406. doi:10.1016/j.hermed.2020.100406
32. Shah B, Davidson PM, Zhong Q. Nanodispersed eugenol has improved antimicrobial activity against Escherichia coli O157: H7 and Listeria monocytogenes in bovine milk. *Int J Food Microbiol*. 2013;161(1):53–59. doi:10.1016/j.ijfoodmicro.2012.11.020
33. Wang Y, Zhou H, Che Y, et al. Emblica officinalis mitigates intestinal toxicity of mice by modulating gut microbiota in lead exposure. *Ecotoxicol Environ Saf*. 2023;253:114648. doi:10.1016/j.ecoenv.2023.114648
34. De Palma G, Lynch MD, Lu J, et al. Transplantation of fecal microbiota from patients with irritable bowel syndrome alters gut function and behavior in recipient mice. *Sci Transl Med*. 2017;9(379):eaaf6397. doi:10.1126/scitranslmed.aaf6397
35. Zeng H, He S, Xiong Z, et al. Gut microbiota-metabolic axis insight into the hyperlipidemic effect of lotus seed resistant starch in hyperlipidemic mice. *Carbohydr Polym*. 2023;314:120939. doi:10.1016/j.carbpol.2023.120939
36. Zhou S-X, Wang L-P, Liu M-Y, et al. Characteristics of diarrheagenic Escherichia coli among patients with acute diarrhea in China, 2009–2018. *J Infect*. 2021;83(4):424–432. doi:10.1016/j.jinf.2021.08.001
37. Ding K, Tan YY, Ding Y, et al. β-Sitosterol improves experimental colitis in mice with a target against pathogenic bacteria. *J Cell Biochem*. 2019;120(4):5687–5694. doi:10.1002/jcb.27853
38. Qu Y, Li X, Xu F, et al. Kaempferol alleviates murine experimental colitis by restoring gut microbiota and inhibiting the LPS-TLR4-NF-κB axis. *Front Immunol*. 2021;12:679897. doi:10.3389/fimmu.2021.679897
39. Shen L, Weber CR, Raleigh DR, Yu D, Turner JR. Tight junction pore and leak pathways: a dynamic duo. *Annu Rev Physiol*. 2011;73(1):283–309. doi:10.1146/annurev-physiol-012110-142150
40. Xiao L, Cui T, Liu S, et al. Vitamin A supplementation improves the intestinal mucosal barrier and facilitates the expression of tight junction proteins in rats with diarrhea. *Nutrition*. 2019;57:97–108. doi:10.1016/j.nut.2018.06.007

41. Ni Y, Zhang Y, Zheng L, et al. Bifidobacterium and Lactobacillus improve inflammatory bowel disease in zebrafish of different ages by regulating the intestinal mucosal barrier and microbiota. *Life Sci*. 2023;324:121699. doi:10.1016/j.lfs.2023.121699
42. Wang D, Zeng J, Wujin C, Ullah Q, Su Z. Lactobacillus reuteri derived from horse alleviates Escherichia coli-induced diarrhea by modulating gut microbiota. *Microb Pathog*. 2024;188:106541. doi:10.1016/j.micpath.2024.106541
43. Tapia R, Kralicek SE, Hecht GA. Modulation of epithelial cell polarity by bacterial pathogens. *Ann NY Acad Sci*. 2017;1405(1):16–24. doi:10.1111/nyas.13388
44. Zhao L, Luo L, Jia W, et al. Serum diamine oxidase as a hemorrhagic shock biomarker in a rabbit model. *PLoS One*. 2014;9(8):e102285. doi:10.1371/journal.pone.0102285
45. Guo G, Shi F, Zhu J, et al. Piperine, a functional food alkaloid, exhibits inhibitory potential against TNBS-induced colitis via the inhibition of IκB-α/NF-κB and induces tight junction protein (claudin-1, occludin, and ZO-1) signaling pathway in experimental mice. *Hum Exp Toxicol*. 2020;39(4):477–491. doi:10.1177/0960327119892042
46. Wang W, Zhang Y, Wang X, Che H, Zhang Y. Piperine improves obesity by repairing intestinal barrier function and inhibiting fatty acid absorption. *Plant Foods for Human Nutrition*. 2021;76(4):410–418. doi:10.1007/s11130-021-00919-2
47. Wang K, Chen D, Yu B, et al. Eugenol alleviates transmissible gastroenteritis virus-induced intestinal epithelial injury by regulating NF-κB signaling pathway. *Front Immunol*. 2022;13:921613. doi:10.3389/fimmu.2022.921613
48. Zheng S, Zhao X, Huang J, et al. Eugenol alleviates Salmonella Typhimurium-infected cecal injury by modulating cecal flora and tight junctions accompanied by suppressing inflammation. *Microb Pathog*. 2023;179:106113. doi:10.1016/j.micpath.2023.106113
49. Yang W, Cong Y. Gut microbiota-derived metabolites in the regulation of host immune responses and immune-related inflammatory diseases. *Cell mol Immunol*. 2021;18(4):866–877. doi:10.1038/s41423-021-00661-4
50. Li Y, Xia S, Jiang X, et al. Gut microbiota and diarrhea: an updated review. *Front Cell Infect Microbiol*. 2021;11:625210. doi:10.3389/fcimb.2021.625210
51. Ma Y, Zhang Q, Liu W, et al. Preventive effect of depolymerized sulfated galactans from eucheuma serra on enterotoxigenic Escherichia coli-caused diarrhea via modulating intestinal flora in mice. *Mar Drugs*. 2021;19(2):80. doi:10.3390/md19020080
52. Chen C, Yue Y, He Z, et al. Lactobacillus gasseri relieves diarrhea caused by enterotoxin-producing Escherichia coli through inflammation modulation and gut microbiota regulation. *Food Bioscience*. 2023;56:103186. doi:10.1016/j.fbio.2023.103186
53. Bai X, Fu R, Duan Z, Liu Y, Zhu C, Fan D. Ginsenoside Rh4 alleviates antibiotic-induced intestinal inflammation by regulating the TLR4-MyD88-MAPK pathway and gut microbiota composition. *Food funct*. 2021;12(7):2874–2885.
54. Zhang W, Ho C-T, Wei W, Xiao J, Lu M. Piperine regulates the circadian rhythms of hepatic clock gene expressions and gut microbiota in high-fat diet-induced obese rats. *Food Science and Human Wellness*. 2024;13(3):1617–1627. doi:10.26599/FSHW.2022.9250137
55. Li M, Zhao Y, Wang Y, et al. Eugenol, a major component of clove oil, attenuates adiposity, and modulates gut microbiota in high-fat diet-fed mice. *mol Nutr Food Res*. 2022;66(20):2200387.
56. Li J, Feng S, Wang Z, et al. Limosilactobacillus mucosae-derived extracellular vesicles modulates macrophage phenotype and orchestrates gut homeostasis in a diarrheal piglet model. *NPJ Biofilms Microbiomes*. 2023;9(1):33. doi:10.1038/s41522-023-00403-6
57. Ma Z-J, Wang H-J, X-j M, et al. Modulation of gut microbiota and intestinal barrier function during alleviation of antibiotic-associated diarrhea with Rhizoma Zingiber officinale (Ginger) extract. *Food Funct*. 2020;11(12):10839–10851. doi:10.1039/D0FO01536A
58. Gomes TA, Elias WP, Scaletsky IC, et al. Diarrheagenic escherichia coli. *Braz J Microbiol*. 2016;47(Suppl 1):3–30. doi:10.1016/j.bjm.2016.10.015